Proc. Natl. Acad. Sci. USA
Vol. 82, pp. 109–113, January 1985
Cell Biology

Immunophotoelectron microscopy: The electron optical analog of immunofluorescence microscopy

(photoelectron imaging/microtubules/colloidal gold/CV-1 epithelial cells)

G. BRUCE BIRRELL*, DOUGLAS L. HABLISTON*, KAREN K. NADAKAVUKAREN†, AND O. HAYES GRIFFITH*

*Institute of Molecular Biology and Department of Chemistry, University of Oregon, Eugene, OR 97403; and †Dana-Farber Cancer Institute and Department of Pathology, Harvard Medical School, 44 Binney Street, Boston, MA 02115

ABSTRACT **The electron optical analog of immunofluorescence microscopy combines three developments: (*i*) photoelectron microscopy to produce a high-resolution image of exposed components of the cell, (*ii*) site-specific antibodies, and (*iii*) photoemissive markers coupled to the antibodies to make the distribution of sites visible. This approach, in theory, provides a way to extend the useful immunofluorescence microscopy technique to problems requiring much higher resolution. The resolution limit of fluorescence microscopy is limited to about 200 nm by the wavelength of the light used to form the image, whereas in photoelectron microscopy the image is formed by electrons (current resolution: 10–20 nm; theoretical limit: 5 nm or better depending on the electron optics). As a test system, cytoskeletons of CV-1 epithelial cells were prepared under conditions that preserve microtubules, and the microtubule networks were visualized by both indirect immunofluorescence and immunophotoelectron microscopy using colloidal gold coated with antibodies. Colloidal gold serves as a label for immunophotoelectron microscopy, providing enhanced photoemission from labeled cellular components so that they stand out against the darker background of the remaining unlabeled structures. In samples prepared for both immunofluorescence and immunophotoelectron microscopy, individual microtubules in the same cells were visualized by both techniques. The photoemission of the colloidal gold markers is sufficiently high that the microtubules are easily recognized without reference to the immunofluorescence micrographs, indicating that this approach can be used, in combination with antibodies, to correlate structure and function in cell biological studies.**

The success of immunofluorescence microscopy in studies of the spatial distribution, function, and interrelationships of cell components is due largely to contrast rather than resolution. The fluorescence microscope is essentially a conventional optical microscope. The high contrast is a result of operating in the emission mode—that is, by small objects giving off light (fluorescing) against a dark background rather than by optical absorption or scattering against a bright field. Combining this high contrast provided by fluorescence emission with the specificity of antibodies, a wealth of information is being obtained about actin-containing structures, microtubules, intermediate filaments, and, indeed, most components of cells and tissues (1–3). As more detailed questions about structure–function relationships are being asked, the resolution limitation (200 nm) of this technique is becoming more troublesome. Higher resolution can be obtained by transmission or scanning electron microscopy combined with electron-dense markers. Although these approaches are valuable, there is still an incentive to retain the emission-type contrast inherent in immunofluorescence and to combine it with the greatly increased resolution provided by electron optics.

The publication costs of this article were defrayed in part by page charge payment. This article must therefore be hereby marked "*advertisement*" in accordance with 18 U.S.C. §1734 solely to indicate this fact.

The electron optical analog of immunofluorescence microscopy utilizes emitted electrons instead of emitted light. The excitation source is still an UV lamp but the optical microscope is replaced by an electron emission-type microscope (photoelectron microscope). The resolution is determined not by the excitation source but by the wavelength of the emitted particle—in this case, a low-energy electron. A comparison of immunofluorescence microscopy and the electron optical analog is shown in Fig. 1. In immunofluorescence, light incident on the biological specimen stimulates fluorescence emission from dye molecules (e.g., fluorescein or rhodamine) that are covalently linked to antibody molecules (Fig. 1 *Left*). In immunophotoelectron microscopy, light of somewhat shorter wavelength stimulates the emission of electrons from suitable markers also linked to antibody molecules (Fig. 1 *Right*). The theoretical resolution of the photoelectron microscope using conventional electron optics is about 5 nm so that the image contains information on the order of single protein resolution (and using corrected electron optics the resolution could approach the diffraction limit of 1 nm for a 1-eV electron). The electrons are then accelerated to high velocities (30–50 kV) and imaged by an electron optical system that gathers information from all emitting points on the specimen simultaneously to form the image. Immunophotoelectron microscopy was first proposed in 1972 (4). Three developments were needed to bring this idea to fruition: the development of a high-resolution ultra-high vacuum photoelectron microscope with image intensification (5), theory and experiments on the photoelectric behavior of biological macromolecules (6–9), and a search for suitable photoemissive markers (10–12). While this work was progressing two important developments, the production of monoclonal antibodies (13) and the introduction of colloidal gold as a marker in electron microscopy (14), have extended the capabilities of immunological mapping approaches, including immunophotoelectron microscopy. In this paper we present a comparison of immunophotoelectron microscopy with immunofluorescence on the same specimens, using, as an example, microtubules in CV-1 epithelial cells.

MATERIALS AND METHODS

Cell Line and Antibodies. CV-1 (African green monkey) kidney epithelial cells were grown on sterile tin oxide-coated 5-mm glass coverslips (Bellco Glass) prepared as described (15). The cells were cultured in Dulbecco's modified Eagle's medium (GIBCO) containing 10% fetal bovine serum (GIBCO), 25 mM Hepes, and 2 mM L-glutamine in a 10% CO_2/90% air incubator at 37°C. The mouse monoclonal IgM antibodies recognizing microtubules were a gift from L. B. Chen. Rhodamine-conjugated goat anti-mouse IgM (GAM) and the rabbit anti-goat IgG (RAG) were obtained from Cappel Laboratories (Cochranville, PA) and E-Y Laboratories (San Mateo, CA), respectively.

Abbreviations: DTSP, dithiobis(succinimidyl propionate); RAG, rabbit anti-goat IgG; GAM, goat anti-mouse IgM.

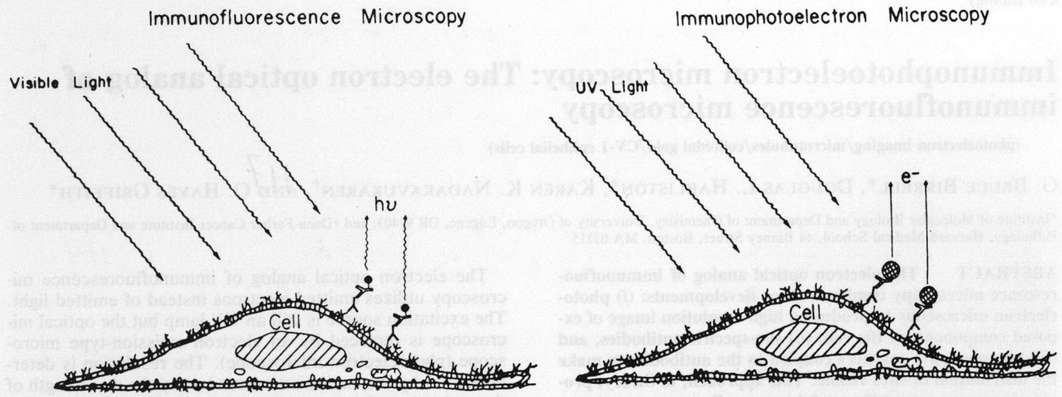

FIG. 1. Schematic diagram of an immunofluorescence experiment (*Left*) and the corresponding immunophotoelectron experiment (*Right*). In both cases markers have been coupled to antibodies directed against a cell surface antigen. In immunofluorescence, the emitted photons mark the distribution of antigen and in immunophotoelectron microscopy, emitted electrons provide similar information but at much higher spatial resolution. The diagram is not drawn to scale (the markers and cell surface components are much smaller than drawn here).

Colloidal Gold and Immunogold Complexes. Colloidal gold particles, 20 nm and 30 nm in diameter, were prepared by the method of Frens (16). Antibody–colloidal gold complexes were made by the procedures of De Mey *et al.* (17) and were stored at 4°C in 20 mM Tris/0.15 M NaCl/20 mM NaN_3/1% bovine serum albumin, pH 8.2.

Detergent Treatment and Immunolabeling. The cells were treated with dithiobis(succinimidyl propionate) (DTSP, from Pierce) for 5 min at 37°C (18). DTSP was freshly diluted from a 20 mg/ml stock solution in dimethyl sulfoxide to a working concentration of 0.2 mg/ml in warm HEN buffer (100 mM Hepes/1 mM EGTA/0.15 M NaCl, pH 7.4). Following the DTSP treatment, the cells were treated with 1% bovine serum albumin in HEN buffer for 3 min at 37°C to block any unreacted DTSP. The DTSP-treated cells were then rinsed with microtubule stabilization buffer (MTS buffer) as described by Osborn and Weber (19) but without GTP [100 mM Hepes/1 mM EGTA/4% polyethylene glycol (6000 molecular weight), pH 7.0] and incubated for 10 min at 37°C in MTS buffer containing 0.5% Triton X-100. Following a rinse with MTS buffer, the extracted cells were fixed in −20°C methanol for 5 min, rehydrated in HEN buffer, and then treated with normal rabbit serum for 20 min at 37°C to reduce nonspecific binding. Antibodies were applied as follows. The first antibody was a murine monoclonal IgM recognizing microtubules, applied as undiluted conditioned medium from hybridoma lines H3-45 or H2-1B2. The second antibody was either rhodamine GAM or rhodamine GAM bound to colloidal gold particles. Where used, the third antibody was RAG bound to 20-nm gold. Incubations for first, second, and third antibodies were 60 min, 30 min, and 2 hr at 37°C, respectively. Several HEN buffer rinses followed each antibody incubation, and the final treatment in all cases was overnight fixation at 4°C in 2.5% glutaraldehyde in HEN buffer.

Fluorescence Microscopy. Samples were mounted by placing the coverslip cell side up on a glass slide. A drop of glycerol containing 0.25 M *n*-propyl gallate to reduce photobleaching (20) was applied to the tin oxide-coated sample mount and a no. 1 glass coverslip was placed over the cells to form a sandwich. This mounting method allows the use of higher resolution oil immersion objectives while protecting the cells for subsequent photoelectron microscopy. Fluorescence microscopy of the rhodamine-labeled cell samples was carried out with epifluorescence excitation at 546 nm on a Zeiss fluorescence microscope equipped with a Zeiss 100× oil immersion objective lens. Exposures were made on Kodak Tri-X film and exposure times were typically 30 sec.

Photoelectron Microscopy. After the fluorescence microscopy, the labeled cell samples were washed with distilled water and then dehydrated through a series of aqueous ethanol mixtures beginning with 70% ethanol followed by critical point drying from CO_2.

The photoelectron microscope used in this study was built at the University of Oregon. It is an ultra-high vacuum instrument designed to eliminate sample contamination and has been described previously (5). The acceleration voltage was 30 kV; the illumination was provided by two OSRAM HBO 100 W/2 Hg short-arc lamps, and the objective aperture was 50 μm. Photoelectron micrographs can be recorded immediately after switching on the UV lamps, but typically the specimens are exposed to the UV light for periods of 5–30 min before recording the images on film in order to take advantage of the gradual increase in image brightness with UV dose (21). There was no change in features of the image, other than brightness, which indicates that the UV irradiation does not cause any gross structural alterations of the specimen during the observation times. The emulsion used was Kodak electron image film 4489; the exposure times varied from 2 to 30 sec.

RESULTS

Fig. 2*A* is a typical immunofluorescence image of microtubule networks in a CV-1 cell. The cell has been extracted with Triton X-100 in a MTS buffer, followed by a three-step antibody application to allow both immunofluorescence (Fig. 2*A*) and immunophotoelectron (Fig. 2*B*) microscopy of microtubules in the same cell. The first, second, and third antibodies were monoclonal IgM recognizing microtubules, rhodamine-conjugated GAM, and RAG bound to 20-nm colloidal gold, respectively. The photoelectron label, in this case the colloidal gold with the third antibody (RAG) bound to it, does not contribute to, nor interfere with, the fluorescence image. Similarly, the rhodamine fluorochrome on the second antibody does not significantly affect the photoelectron image (15). The gold-labeled microtubules are clearly visible in Fig. 2*B*, even though at this relatively low magnification the individual gold particles are barely discernible.

Microtubules have a diameter of 25 nm. The fibers being imaged, however, are much thicker because they have been coated with one layer of IgM (20 nm), a second layer of fluorescently labeled IgG (9 nm), and a third layer composed of IgG adsorbed to 20-nm diameter colloidal gold. The fluorescence image arises from the second antibody layer surrounding the microtubules and the photoemission image originates from the third and final layer containing the colloidal gold. On this basis alone the fibers seen in the fluorescence micrograph would be smaller in diameter than those of the corresponding photoelectron micrograph. However, just the opposite occurs because the resolution in the photoelectron micrograph is much greater. The microtubules in Fig. 2*A* are imaged at the resolution of the fluorescence microscope (200 nm), whereas the fibers in the photoelectron microscope are resolved at more nearly their true dimensions, as long as the physical dimensions of the objects are at least as great as the current resolution of the instrument (10–20 nm). Measurements on specimens prepared by the three-step procedure, but without the gold, indicate an average diameter of about 70 nm for the antibody-coated microtubules.

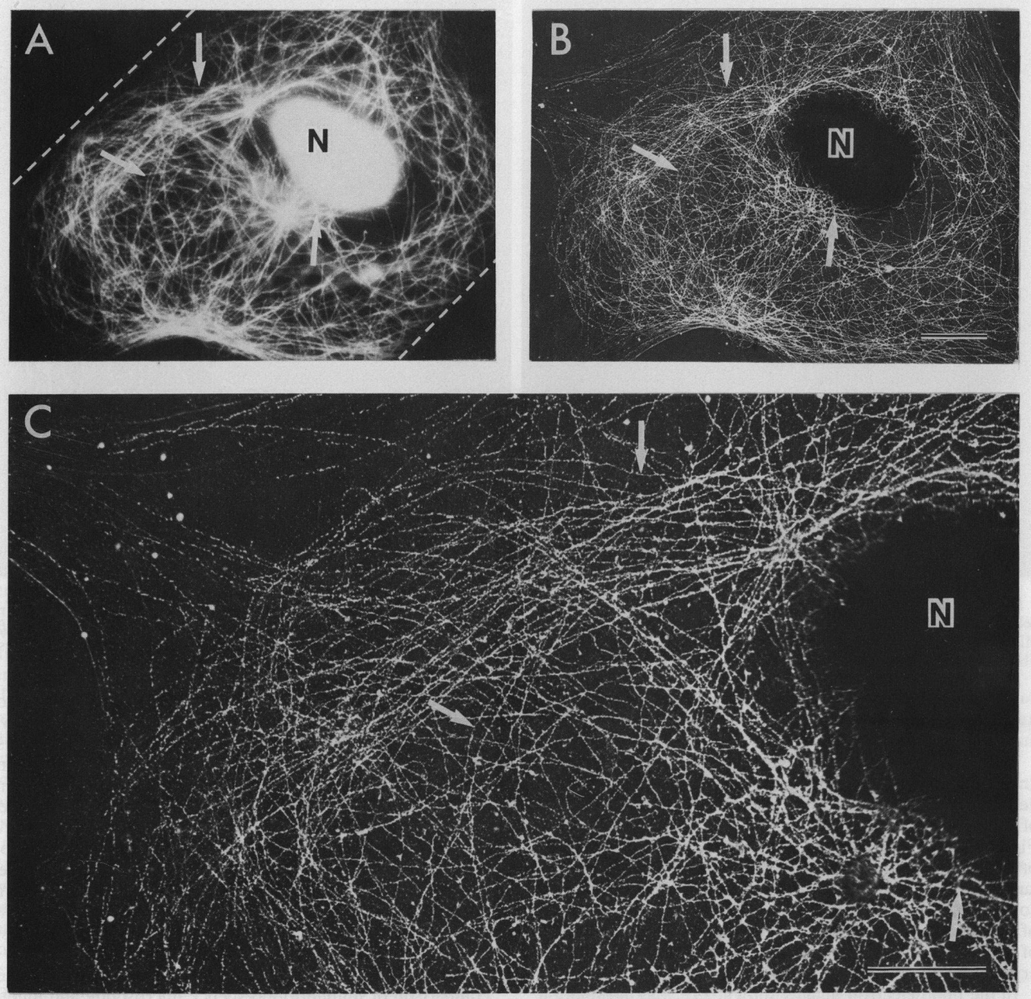

FIG. 2. Comparison of an immunofluorescence micrograph (*A*) of a cell prepared for the visualization of microtubules with an immunophotoelectron micrograph (*B*) of the same cell after critical point drying. (*C*) A 5× enlargement of *B*. A three-step, double-labeling procedure was used so that the microtubules were labeled with both a fluorescent marker (rhodamine) and a photoelectron marker (20-nm colloidal gold). Arrows identify some of the many microtubules that can be seen in both the fluorescence and photoelectron micrographs. The diagonal dashed lines in *A* indicate the edges of the micrograph after rotation so that the cell has the same orientation as in *B* and *C*. N, nucleus. (Bars are 10 and 5 μm for *B* and *C*, respectively.)

Fig. 3 *A* and *B* are immunophotoelectron micrographs of CV-1 cells prepared as above, except that only a two-step antibody procedure was used in order to minimize the layers of antibody coating the microtubules. In this experiment, the second antibody rather than a third antibody was bound to the colloidal gold label. Although the second antibody used here was the same rhodamine GAM as used in the experiment of Fig. 2, the amount of fluorescence was insufficient to provide good-quality immunofluorescence images. However, the immunophotoelectron micrographs of Fig. 3 *A* and *B* clearly illustrate the distribution of microtubules in this cell, with minimal nonspecific binding. Other two-step labeling experiments in which the second antibody carried only the gold label and not the rhodamine fluorochrome gave sim-

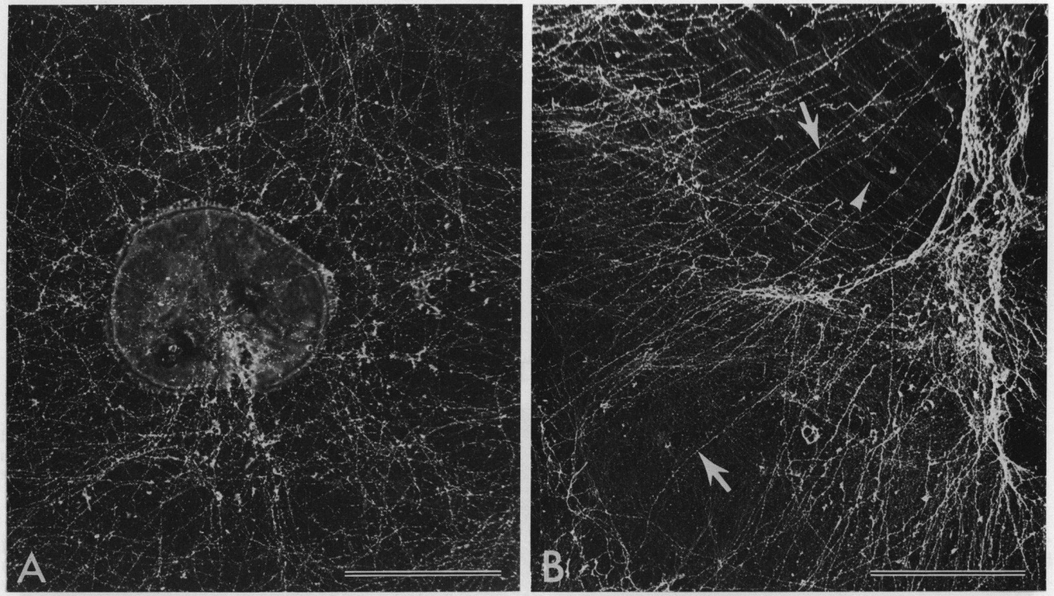

FIG. 3. Immunophotoelectron micrographs showing contrast between labeled and unlabeled cellular components. (*A*) Micrograph of a CV-1 cell prepared for the visualization of microtubules using a two-step procedure with 20-nm colloidal gold as the photoemissive marker; (*B*) Micrograph of another CV-1 cell prepared in the same way showing microtubules labeled with 30-nm gold against a field of unlabeled stress fibers. Representative labeled microtubules (arrows) and actin-containing stress fibers (arrowhead) are identified. (Bars are 10 μm.)

ilar results, confirming that the primary source of label contrast in the photoelectron images is provided by the gold markers.

The image of the nuclear region in photoelectron micrographs depends on the topography and amount of cellular debris remaining on top of the nucleus. We find a variation of the image quality of the nuclear region. For example, in Fig. 2 *B* and *C* the nuclear region is dark and unresolved, presumably due to greater topography or unextracted cellular debris, whereas in Fig. 3*A* the nuclear region is well resolved and brighter, and the two nucleoli can be seen. Some of the labeled microtubules can be traced across the surface of the nucleus while others disappear at the nuclear boundary, evidently proceeding under the nucleus.

In the photoelectron images shown here, the information is a function of the sample surface itself and not of staining, shadowing, or coating with metals to provide contrast and conductivity. The images are formed from the electrons photoejected from the native (fixed) or labeled cellular components under the action of UV light. These photoelectrons are produced in sufficient numbers in both the presence and absence of markers to form a detectable image.

DISCUSSION

In studies of complex biological structures, two sources of information are desirable: (*i*) markers to identify the distribution of specific proteins and (*ii*) a high-resolution topographical map of the biological structure. The great usefulness of immunofluorescence microscopy lies in the markers: antibodies coupled to dye molecules that emit light. These markers are easily seen against the darker background of the cell and are therefore useful in identifying distributions of antigenic sites. The strategy in immunophotoelectron microscopy as diagrammed in Fig. 1 is to retain the concept of emission against the darker unlabeled surface but to utilize electron emission in place of photon emission to increase the spatial resolution.

We selected collodial gold as an initial marker for immunophotoelectron microscopy because of its photoemissive properties (22). Although materials that are more photoemissive exist, colloidal gold is enjoying wide use as an electron-dense marker for transmission electron microscopy and scanning electron microscopy and can be seen in some cases by optical microscopy (14, 17). There have even been a few reports of double-labeling for fluorescence and transmission electron microscopy using fluorescent protein conjugates coupled to colloidal gold (23, 24), although not the specific combination used here. Thus, at present colloidal gold comes closest to being a universal marker and makes possible a wide range of comparative experiments.

The double-labeling experiment of Fig. 2 provides a direct comparison of immunofluorescence microscopy and immunophotoelectron microscopy on the same specimen. The network of microtubules is visible in both micrographs, Fig. 2 *A* and *B*. The arrow marks one such fiber, but many more can be traced in these two micrographs. The striking contrast of labeled microtubules against the background is more clearly seen in the enlargement of the immunophotoelectron micrograph of Fig. 2*C* and in Fig. 3. The microtubules radiate outwards from what appear to be microtubule-organizing centers just to the left and near the top of the nucleus in Fig. 2.

In correlating structure and function it is desirable to visualize individual markers because each one, depending on the design of the experiment, can represent a single antibody and thus a single antigenic site. In immunofluorescence it is not in general possible to discern single sites even though the contrast is relatively high. The present results show that it is possible to image single markers by immunophotoelectron microscopy. In Fig. 2*C* and Fig. 3 individual 20-nm gold particles are easily seen as bright dots against the unlabeled background. Thus, it does not require a specific density of colloidal gold particles to form one image point, as in fluorescence microscopy. There are reports in the physics literature that small particles exhibit enhanced photoemission compared to uniform layers of the same substances (25), and continued work in this field will help provide a theoretical basis for selecting the optimal diameters and materials for photoelectron microscopy markers.

In addition to imaging labeling patterns, photoelectron imaging provides topographical contrast necessary to relate the spatial distribution of labeled structures to the distribution of other, unlabeled, cellular components. This is illustrated most clearly in Fig. 3. Fig. 3*B* demonstrates that both labeled and unlabeled cytoskeletal elements can be detected in the same field of view. The microtubules stand out because of the photoemissive gold markers, and the actin-containing stress fibers and other filaments are visible because of the topographical contrast. There is no ambiguity in distinguishing between the labeled and unlabeled fibers. The ability to image both at the same time is consistent with the theory of photoelectron imaging.

Topographical contrast in photoelectron imaging is provided by the deflection of the initially slow-moving electrons as they are emitted from or near three-dimensional structures on the specimen surface (9). This sensitivity to topographical detail is very useful for imaging fine details but can exceed the useful range in cases of larger-scale structures, such as some nuclear regions and rounded-up cells. Topographical contrast has been used alone to visualize cytoskeletal structures by photoelectron imaging in a previous study (15). In that case, the cytoskeletal elements were indirectly identified by comparison with immunofluorescence images of the same cells. The present study represents a significant advance in that photoelectron markers bound to site-specific antibodies are used to directly identify specific cytoskeletal elements.

To summarize, the purpose of the present study is to demonstrate the use of photoelectron imaging in conjunction with antibody techniques as the electron optical analog of immunofluorescence microscopy. Immunophotoelectron microscopy employs both photoemissive markers and topographical information to provide an image of the distribution of specific antigenic sites with respect to cellular structures. Immunophotoelectron microscopy retains the essential basis of immunofluorescence—that is, the emission of signals from markers against a darker background. Beyond this formal analogy, there are significant differences in image formation and applications. Immunofluorescence microscopy can be used on live or wet specimens, for example, whereas the electron microscope methods, including photoelectron imaging, generally require the specimen to be either dehydrated or frozen. Photoelectron microscopy has been compared with transmission electron microscopy and scanning electron microscopy elsewhere (8). Immunophotoelectron microscopy will not replace the existing microscope techniques but it has the potential of contributing valuable additional information because it has an extremely high surface sensitivity (short escape depths), has high topographic contrast, and requires no coating of the biological surface.

We thank Drs. Lan Bo Chen, Gertrude F. Rempfer, and Patricia J. Harris for encouragement and useful discussions and Walter K. Skoczylas for continued improvements in the University of Oregon photoelectron microscope. This work was supported by Grant CA-11695 from the National Cancer Institute and a grant from the M. J. Murdock Charitable Trust. K.K.N. is the recipient of a National Cancer Institute Postdoctoral Fellowship (CA-070407-02).

1. Osborn, M., Webster, R. E. & Weber, K. (1978) *J. Cell Biol.* **77,** R27–R34.
2. Lazarides, E. (1980) *Nature (London)* **283,** 249–256.
3. Brinkley, B. R., Fistel, S. H., Marcum, J. M. & Pardue, R. L. (1980) *Int. Rev. Cytol.* **63,** 59–95.
4. Griffith, O. H., Lesch, G. H., Rempfer, G. F., Birrell, G. B., Burke, C. A., Schlosser, D. W., Mallon, M. H., Lee, G. B., Stafford, R. G., Jost, P. C. & Marriott, T. B. (1972) *Proc. Natl. Acad. Sci. USA* **69,** 561–565.
5. Griffith, O. H., Rempfer, G. F. & Lesch, G. H. (1981) *Scanning Elec. Microsc.* **2,** 123–130.
6. Dam, R. J., Nadakavukaren, K. K. & Griffith, O. H. (1977) *J. Microsc. (Oxford)* **111,** 211–217.
7. Houle, W. A., Engel, W., Willig, F., Rempfer, G. F. & Griffith, O. H. (1982) *Ultramicroscopy* **7,** 371–380.
8. Griffith, O. H., Rempfer, G. F. & Nadakavukaren, K. K. (1982) in *Electron Microscopy 1982: Proceedings of the Tenth International Congress on Electron Microscopy*, ed. Le Poole, J. B. (Deutsche Gesellschaft für Electronenmikroskopie, e.V., Frankfurt), Vol. 1, pp. 59–68.
9. Rempfer, G. F., Nadakavukaren, K. K. & Griffith, O. H. (1980) *Ultramicroscopy* **5,** 437–448.
10. Birrell, G. B., Burke, C., Dehlinger, P. & Griffith, O. H. (1973) *Biophys. J.* **13,** 462–469.
11. Dam, R. J., Kongslie, K. F. & Griffith, O. H. (1974) *Biophys. J.* **14,** 933–939.
12. Griffith, O. H. & Birrell, G. B. (1983) *Proc. Elec. Microsc. Soc. Am.* **41,** 510–511.
13. Köhler, G. & Milstein, C. (1975) *Nature (London)* **256,** 495–497.
14. Horisberger, M. & Rosset, J. (1977) *J. Histochem. Cytochem.* **25,** 295–305.
15. Nadakavukaren, K. K., Chen, L. B., Habliston, D. L. & Griffith, O. H. (1983) *Proc. Natl. Acad. Sci. USA* **80,** 4012–4016.
16. Frens, G. (1973) *Nat. Phys. Sci.* **241,** 20–22.
17. De Mey, J., Moeremans, M., Geuens, G., Nuydens, R. & De Brabander, M. (1981) *Cell Biol. Int. Rep.* **5,** 889–899.
18. Bell, P., Jr. (1981) *Scanning Elec. Microsc.* **2,** 139–157.
19. Osborn, M. & Weber, K. (1977) *Cell* **12,** 561–571.
20. Giloh, H. & Sedat, J. W. (1982) *Science* **217,** 1252–1255.
21. Griffith, O. H., Holmbo, D. L., Habliston, D. L. & Nadakavukaren, K. K. (1981) *Ultramicroscopy* **6,** 149–156.
22. Birrell, G. B., Rose, S. M. & Griffith, O. H. (1983) *Ultramicroscopy* **12,** 213–218.
23. Horisberger, M. & Vonlanthen, M. (1979) *Histochemistry* **64,** 115–118.
24. Roth, J., Bendayan, M. & Orci, L. (1980) *J. Histochem. Cytochem.* **28,** 55–57.
25. Penn, D. R. & Rendell, R. W. (1981) *Phys. Rev. Lett.* **47,** 1067–1070.